

Scaling behavior of charged hadron p_T distributions in pp and $p\bar{p}$ collisions

W. C. Zhang^{1*} and C. B. Yang^{2†}

¹*School of Physics and Information Technology, Shaanxi Normal University, Xi'an 710062, China*

²*Key Laboratory of Quark and Lepton Physics (MOE) and Institute of Particle Physics, Central China Normal University, Wuhan 430079, China*

(Dated: March 24, 2014)

We present that there is a scaling behavior in the transverse momentum (p_T) distributions for charged hadrons produced in proton-proton (pp) collisions with different center of mass energy scales ($\sqrt{s} = 0.9, 2.36$ and 7 TeV) at the Compact Muon Solenoid (CMS) detector. A similar scaling behavior is observed in the p_T distributions of charged hadrons produced in proton-antiproton ($p\bar{p}$) collisions with $\sqrt{s} = 0.63, 1.8$ and 1.96 TeV at the Collider Detector at Fermilab (CDF). The statistics origin of this scaling behavior could be from the non-extensivity of the particle system produced in the collisions. And the particle production mechanism behind the scaling behavior could be explained by the model of percolation of strings.

PACS numbers: 13.85.Ni, 13.87.Fh

I. INTRODUCTION

One of the main goals in high energy collisions is to investigate the dynamics for particle productions. Several approaches are utilized to search for regularities in the particle productions. One of the approaches is to search for a scaling behavior of some quantities versus suitable variables.

The scaling behavior was first introduced in electron-nucleon deep inelastic scattering (DIS) in which the x -scaling of the structure functions exhibit [1]. In recent years, scaling behaviors were observed in nucleus-nucleus collisions. Ref. [2] showed that a scaling behavior exhibited in the pion p_T spectra with different collision centralities at midrapidity in Au+Au collisions at the Relativistic Heavy Ion Collider (RHIC). This scaling behavior of pions was also found in noncentral regions in Au+Au and d+Au collisions [3]. An analogous scaling behavior was observed in the proton and anti-proton p_T spectra with different collision centralities at midrapidity in Au+Au collisions at RHIC [4].

Recently, a universal scaling behavior was presented in the p_T distributions of charged hadrons in pp collisions with $\sqrt{s}=0.9, 2.36$ and 7 TeV at CMS [5]. This scaling behavior is seen when the p_T distributions are in a suitable variable, p'_T . p'_T at energy scale \sqrt{s} is defined in terms of p_T at energy scale \sqrt{s} and it is written as $p'_T = p_T(\sqrt{s}/\sqrt{s})^{\frac{\lambda}{\lambda+2}}$, where λ is a parameter and it depends on p_T at energy scale \sqrt{s} . Ref. [6] showed that this scaling behavior could be described by a Tsallis distribution [7]. In this paper, we propose another method to search for the scaling behavior of the charged hadron p_T distributions in pp collisions with $\sqrt{s} = 0.9, 2.36$ and 7 TeV. This scaling behavior exhibits when the p_T distributions are presented in another suitable variable,

$z = p_T/K$. Here K is a free parameter which only depends on \sqrt{s} , rather than p_T at energy scale \sqrt{s} . This scaling behavior could be described by an exponential distribution. Similar scaling behavior is also searched for in the charged hadron p_T distributions in $p\bar{p}$ collisions with $\sqrt{s} = 0.63, 1.8$ and 1.96 TeV at CDF. The scaling behaviors in the pp and $p\bar{p}$ collisions can also be described with Tsallis distributions. We compare the exponential distribution with the Tsallis distribution and find they are in good agreement. This indicates that the particle systems produced in pp and $p\bar{p}$ collisions are non-extensive thermodynamics systems.

This paper is organized as follows. In Sec. II, the procedure to search for the scaling behavior in pp and $p\bar{p}$ collisions is illustrated. Sec. III describes the scaling behavior of charged hadrons in pp and $p\bar{p}$ collisions with different center of mass energy scales. In Sec. IV, the statistic origin of this scaling distribution is studied. Sec. V shows the comparison between the scaling behaviors presented in the variables z and p'_T . Finally in Sec. VI, the possible particle production mechanism behind the scaling behavior is discussed.

II. METHOD TO SEARCH FOR THE SCALING BEHAVIOR

The method to search for the scaling behavior of charged hadron p_T spectra at different energy scales in pp and $p\bar{p}$ collisions is similar to the one which was described in Refs. [2–4]. Here we will describe it briefly. By choosing proper parameters A and K , the scaled p_T spectra at different energy scales in pp or $p\bar{p}$ collisions, $\Phi(z) = A \cdot (2\pi p_T)^{-1} d^2N/dp_T dy|_{p_T=Kz}$, will exhibit a universal scaling behavior. As a convention, K and A are set to be 1 for the highest energy collisions. Obviously, with different choices of A and K for the highest energy collisions, we get different scaling functions. The arbitrary of the scaling function $\Phi(z)$ will disappear if the p_T spectra at different energy scales are pre-

* Electronic address: wenchao.zhang@snnu.edu.cn

† Electronic address: cbyang@mail.ccnu.edu.cn

sented in another variable, $u = z/\langle z \rangle = p_T/\langle p_T \rangle$. Here $\langle z \rangle = \int_0^\infty z \Phi(z) z dz / \int_0^\infty \Phi(z) z dz$. The normalized scaling distribution as a function of u then is defined as $\Psi(u) = \langle z \rangle^2 \Phi(\langle z \rangle u) / \int_0^\infty \Phi(z) z dz$.

III. SCALING BEHAVIOR IN pp AND $p\bar{p}$ COLLISIONS

The charged hadron p_T spectra in pp ($p\bar{p}$) collisions with $\sqrt{s} = 0.9, 2.36$ and 7 ($0.63, 1.8$ and 1.96) TeV at CMS (CDF) were published in Refs. [8–10]. The p_T distributions in CDF data cover a range up to 50 GeV/c, which is larger than the p_T coverage of CMS data. As shown in Fig. 1, these p_T spectra in pp collisions with different energy scales can be put to one curve by choosing suitable parameters A and K . These parameters are tabulated in Table I. The curve is described by an exponential function,

$$\Phi_{pp}(z) = 27.63 \exp(-6.93v + 0.44v^2 - 0.26v^3), \quad (1)$$

where $v = \ln(1 + z)$.

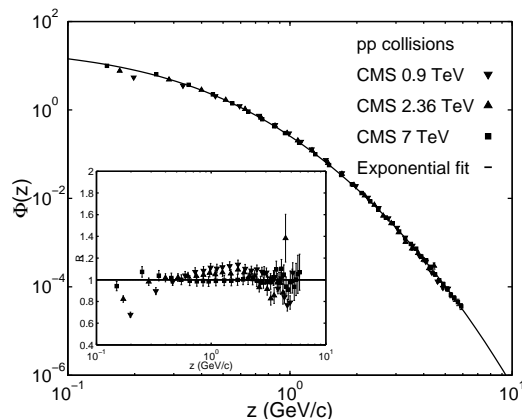


FIG. 1. Scaling behavior of the charged hadron p_T spectra presented in z in the pp collisions with different energy scales. The solid curve is described by Eq. 1. The data points are taken from [8]. The inset shows the distribution of the ratio between the experimental data and the fitted results.

TABLE I. A and K parameters for putting data points in the pp collisions with different energy scales to the curve described in Eq. 1.

\sqrt{s} (TeV)	K	A
0.9	0.76	0.85
2.36	0.88	0.95
7	1	1

In order to see how well the CMS data with different energy scales agree with the fitted curve, we define a

ratio,

$$R = \text{experimental data/fitted results}. \quad (2)$$

The inset of Fig. 1 shows R as a function of z for all data points in the pp collisions with different energy scales. Except for a few data points which lie in the soft or hard region, all the data points have R values in the range 0.8 – 1.2 , which implies that the scaling behavior is true within an accuracy of 20%.

In a similar way, the p_T spectra in the $p\bar{p}$ collisions with different energy scales can be placed to another curve with another set of parameters A and K (see Fig. 2). These parameters are listed in Table II. The curve for the $p\bar{p}$ collisions is described by another exponential function,

$$\Phi_{p\bar{p}}(z) = 1085.12 \exp(-6.56v - 0.64v^2 + 0.12v^3), \quad (3)$$

where v is also defined as $v = \ln(1 + z)$.

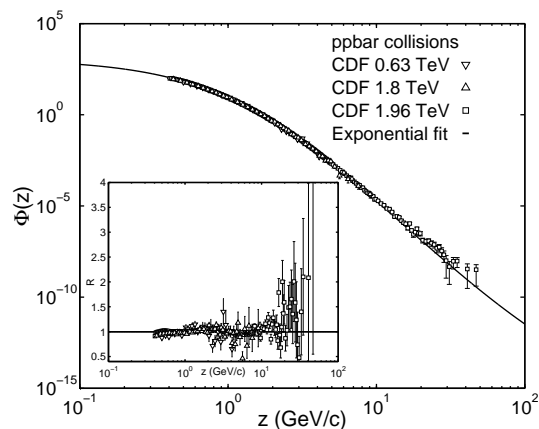


FIG. 2. Scaling behavior of the charged hadron p_T spectra presented in z in the $p\bar{p}$ collisions with different energy scales. The solid curve is described by Eq. 3. The data points are taken from [9, 10]. The inset is the distribution of the ratio between the experimental data and the fitted results.

TABLE II. A and K parameters for putting data points in the $p\bar{p}$ collisions with different energy scales to the curve described in Eq. 3.

\sqrt{s} (TeV)	K	A
0.63	0.85	2.37
1.8	0.99	2.14
1.96	1	1

The R (see Eq. 2) distribution as a function of z for the $p\bar{p}$ collisions is presented in the inset of Fig. 2. In the low p_T region with $z < 10$ GeV/c, the data points and the fitted curve agree within 20%. In the high p_T region with $z > 10$ GeV/c, there is a large deviation between the data points and the fitted curve.

So far we have seen that the charged hadron p_T distributions in the pp and $p\bar{p}$ collisions indeed exhibit a

scaling behavior. However, the scaling functions in Eqs. 1 and 3 rely on the choice of parameters A and K for the highest energy collisions. In order to eliminate this dependence on the choice, the scaling variable z is replaced by $u = z/\langle z \rangle$. In the pp ($p\bar{p}$) collisions, $\langle z \rangle$ for the charged hadrons is determined as 0.53 (0.48) with the definite integral of z over the interval $[0, 10]$ ($[0, 100]$), which roughly corresponds to the p_T range measured by CMS (CDF). Plugging $\langle z \rangle$ as well as $\Phi(z)$ into $\Psi(u)$ defined in Sec. II, one can easily get the normalized scaling function $\Psi_{pp}(u)$ ($\Psi_{p\bar{p}}(u)$) for the pp ($p\bar{p}$) collisions (see Fig. 3). In order to get a similar form of $\Phi(z)$ in Eqs. 1 and 3, $\Psi_{pp}(u)$ and $\Psi_{p\bar{p}}(u)$ are reparameterized as follows:

$$\begin{aligned} \Psi_{pp}(u) &= 7.81 \exp(-3.73v - 0.61v^2 - 0.02v^3) \\ \Psi_{p\bar{p}}(u) &= 5.95 \exp(-2.75v - 1.44v^2 + 0.16v^3) \end{aligned} \quad (4)$$

where $v = \ln(1 + u)$.

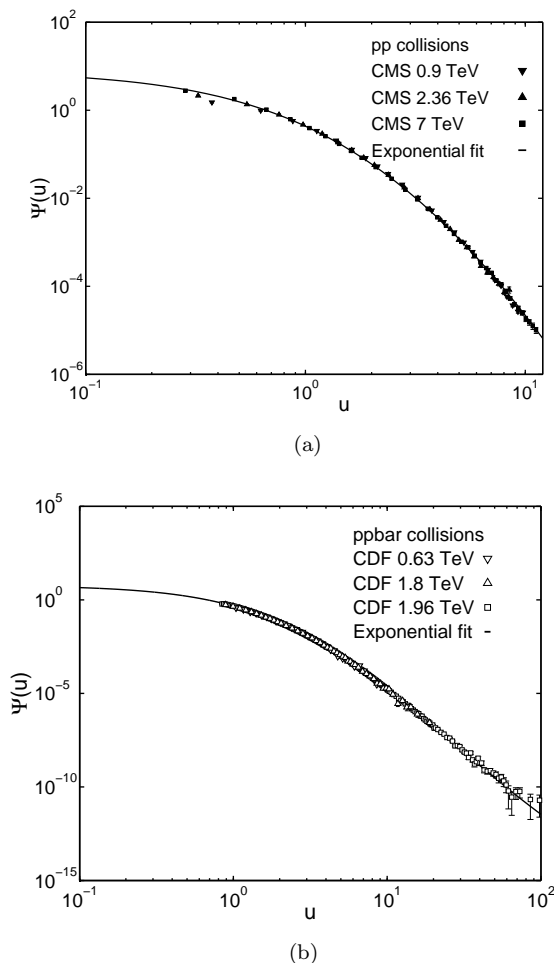


FIG. 3. (a) ((b)), normalized scaling distribution as a function of variable u for the charged hadrons produced in the pp ($p\bar{p}$) collisions. The solid curves are described by Eq. 4. The CMS (CDF) data points are taken from [8] ([9, 10]).

The scaling behavior of the p_T distributions for charged hadrons produced in the pp and $p\bar{p}$ collisions

could be validated experimentally in the following way. With the normalized scaling functions in Eq. 4, we can calculate the ratio between the moments of the momentum distributions,

$$\frac{\langle p_T^n \rangle}{\langle p_T \rangle^n} = \int_0^\infty u^n \Psi(u) u du, \quad (5)$$

where $n = 2, 3, 4, \dots$. The integration interval for $\Psi_{pp}(u)$ ($\Psi_{p\bar{p}}(u)$), which corresponds to the range of $p_T/\langle p_T \rangle$ measured by CMS (CDF), is from 0 to 12 (100). Table III tabulates $\langle p_T^n \rangle / \langle p_T \rangle^n$ with $n = 2, 3, 4, 5$ for the charged hadrons produced in the pp and $p\bar{p}$ collisions. Judging from Eq. 5, $\langle p_T^n \rangle / \langle p_T \rangle^n$ does only depend on the form of the normalized scaling function $\Psi_{pp}(u)$ or $\Psi_{p\bar{p}}(u)$. If the scaling behavior of the charged hadron p_T distributions is true, then the ratio between the moments of momentum should be a constant for collisions with different energy scales. As an example, the ratios between the moments of momentum with $n = 2$ are calculated using the measured data points for the charged hadron p_T distributions in the pp collisions with $\sqrt{s} = 0.9, 2.36$ and 7 TeV, and they are 1.68, 1.73 and 1.85. These experimental values and the value calculated with the integral of the normalized scaling function $\Psi_{pp}(u)$, 1.93, are deemed to be consistent within 20%. This general agreement confirms that the scaling behavior of the charged hadron p_T distributions in the pp collisions with different energy scales is true. We can also test the scaling behavior of the charged hadron p_T distributions in the $p\bar{p}$ collisions with different energy scales experimentally in a similar way.

TABLE III. $\langle p_T^n \rangle / \langle p_T \rangle^n$ calculated with Eq. 5 for the charged hadrons produced in the pp and $p\bar{p}$ collisions.

n	pp collisions	$p\bar{p}$ collisions
2	1.93	1.90
3	6.23	6.39
4	29.93	42.04
5	188.92	663.58

IV. STATISTICS ORIGIN OF THE SCALING BEHAVIOR

We have shown that the scaling behavior of the charged hadron p_T distributions in the pp or $p\bar{p}$ collisions could be described by an exponential distribution in Sec. III. Now we would like to explore the statistic origin of this scaling behavior. The scaling functions in Eqs. 1 and 3 are in an exponential form of v , rather than z , thus the statistical mechanics of the particle production in the pp and $p\bar{p}$ collisions is thought to be non-extensive. As described in Sec. I, the scaling behavior of the p_T distributions presented in the variable p_T in the pp collisions could be described by a Tsallis distribution. We would like to

see whether the scaling behavior of the p_T distributions presented in the variable z could also be described by the Tsallis distribution. The Tsallis distribution [6],

$$\Phi(z) = C_q \left[1 - (1 - q) \frac{z}{z_0} \right]^{\frac{1}{1-q}}, \quad (6)$$

is derived by maximizing the Tsallis entropy, which is a non-extensive entropy. Here C_q is a normalization factor, z_0 and q are free parameters. $|1 - q|$ is a measure of the non-extensivity. When $q \rightarrow 1$, the Tsallis distribution becomes the Boltzmann-Gibbs distribution,

$$\Phi(z) = C_1 \exp\left(-\frac{z}{z_0}\right), \quad (7)$$

which could be revealed from the maximum of the extensive Boltzmann-Gibbs entropy. Fig. 4 shows that the scaling behaviors of p_T distributions presented in z are fitted by Eq. 6. For the pp ($p\bar{p}$) collisions, $C_q=22.04$ (1131.52), $z_0=0.17$ (0.15) and $q=1.127$ (1.125). The inset plots in Fig. 4 show that, except for in the region $z > 10$, the Tsallis curves agree with most of the data points within an accuracy of 20%. This implies that the Tsallis distribution could also depict the scaling behaviors of charged hadron p_T distributions in the pp and $p\bar{p}$ collisions well.

As a result, there are two possible ways to describe the scaling behavior of the charged hadron p_T distributions. In order to see how good is the consistency between these two scaling behavior descriptions, the normalized Tsallis scaling functions for the pp and $p\bar{p}$ collisions,

$$\begin{aligned} \Psi_{pp}^{\text{Tsa.}}(u) &= 6.75 \left[1 - (1 - 1.127) \frac{u}{0.311} \right]^{\frac{1}{1-1.127}} \\ \Psi_{p\bar{p}}^{\text{Tsa.}}(u) &= 6.72 \left[1 - (1 - 1.125) \frac{u}{0.313} \right]^{\frac{1}{1-1.125}} \end{aligned}, \quad (8)$$

are compared to the normalized exponential scaling functions in Eq. 4 at logarithm scale (see Fig. 5). As shown in the inset of Fig. 5(a), the ratio between the two normalized scaling functions for the pp collisions, $B=\text{Tsallis fit}/\text{Exponential fit}$, is constrained in the range $[0.85, 1.1]$, which means that the difference between these two functions is less than 15%. For the $p\bar{p}$ collisions, the normalized Tsallis and exponential distributions are in agreement within 10% when $u < 20$ (see the inset of Fig. 5(b)). When u is greater than 20, the discrepancy between these two distribution starts to grow with u monotonically. This could be due to the reason that at large p_T there are not enough statistics and thus there is a large uncertainty associated with the number of events observed at this p_T region. The agreement between the Tsallis and exponential normalized scaling functions tells us that the charged hadron system produced in the pp ($p\bar{p}$) collisions is a non-extensive thermodynamics systems, and the non-extensivity of the system is described by the parameter q , which is 1.127 (1.125).

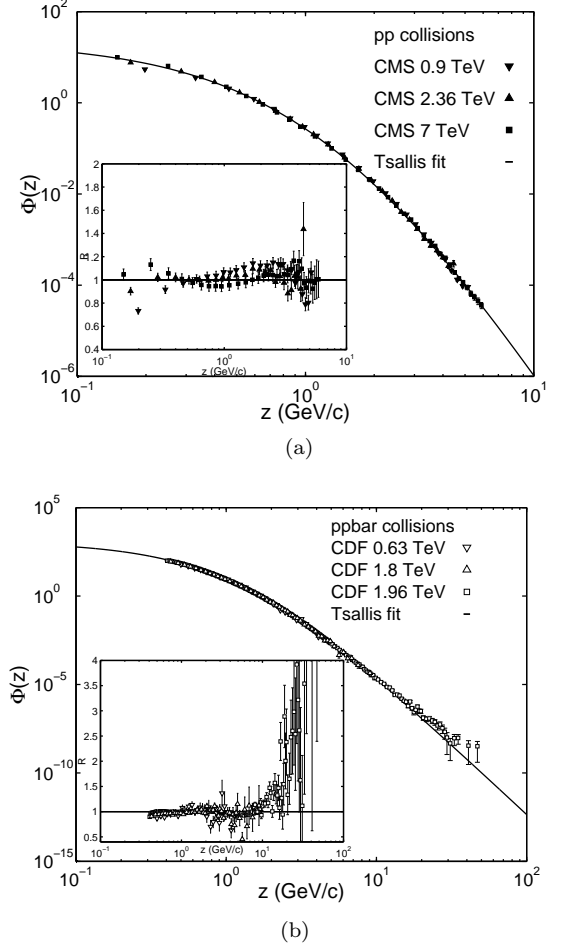


FIG. 4. (a) ((b)), scaling behavior of the charged hadron p_T spectra presented in z in the pp ($p\bar{p}$) collisions. The solid curves are described by Eq. 6. The CMS (CDF) data points are taken from [8] ([9, 10]). The inset is the distribution of the ratio between the experimental data and the fitted results.

V. COMPARISON BETWEEN THE SCALING BEHAVIORS PRESENTED IN z AND p_T

As described in Ref. [5], there is a scaling behavior when the charged hadron p_T spectra in the pp collisions at different energy scales are presented in the variable p_T' . The p_T spectrum at \sqrt{s} is connected with the p_T' at $\sqrt{s'}$ via $p_T' = p_T(\sqrt{s'}/\sqrt{s})^{\frac{\lambda}{\lambda+2}}$, where $\lambda = 0.13 + 0.1(4p_T^2/10)^{0.35}$. Fig. 6 shows the p_T distributions presented in p_T' in the pp collisions for different energy scales. In this figure, the p_T spectra at $\sqrt{s} = 2.36$ and 0.9 TeV have been rescaled to the p_T' spectrum at $\sqrt{s'} = 7$ TeV. The latter spectrum is described by an exponential fit in Eq. 1. The inset of Fig. 6 shows the distribution of the ratio between the experimental data and the fitted results. Except a few data points at high p_T region, the scaling behavior of the charged hadron p_T spectra presented in p_T' is true within an accuracy of 50%. As

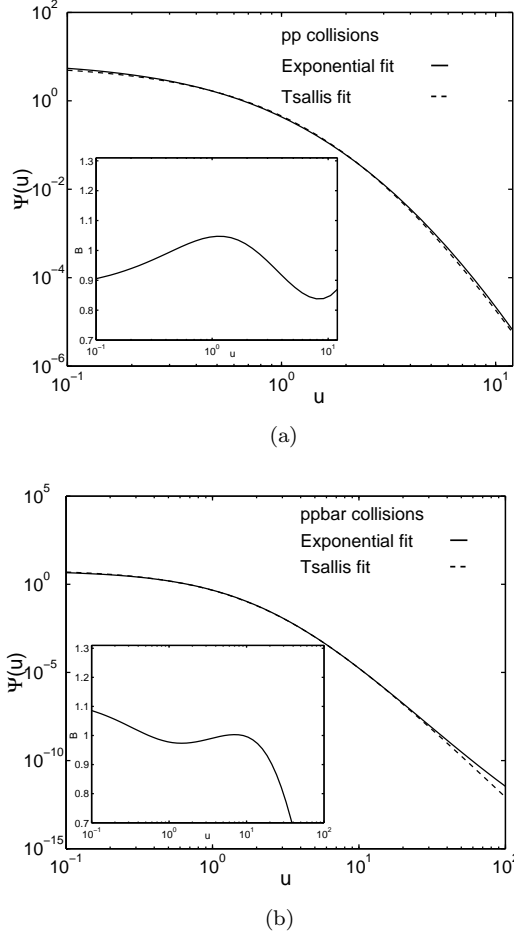


FIG. 5. (a) ((b)), comparison between the normalized Tsallis and exponential scaling functions of charged hadrons in the pp ($p\bar{p}$) collisions. The inset presents the distribution of the ratio between these two normalized scaling functions.

described in Sec. III, the truth of the scaling behavior of the charged hadron p_T spectra presented in z in the pp collisions with different energy scales is within an accuracy of 20%. As a result, the scaling behavior of the charged hadron p_T spectra presented in z is more obvious than the one presented in p_T .

VI. DISCUSSIONS

We have shown that there is a scaling behavior in the p_T distributions of charged hadrons produced in the pp or $p\bar{p}$ collisions with different energy scales. This scaling behavior is observed when a linear transformation is applied on p_T . The exponential and Tsallis distributions can both be applied to describe this scaling behavior within an accuracy of 20%. The agreement between these two distributions shows that the particle systems in the pp and $p\bar{p}$ collisions are non-extensive thermodynamics systems. In order to understand the particle production

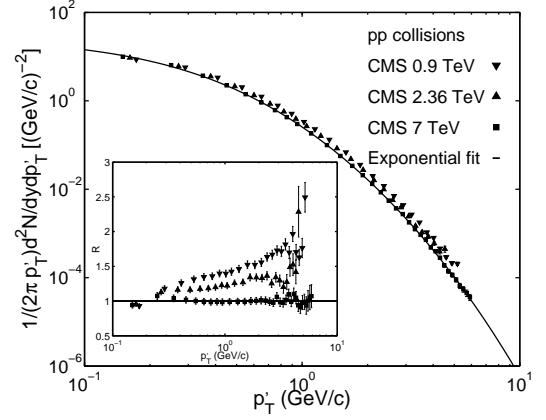


FIG. 6. Scaling behavior of the charged hadron p_T spectra presented in p_T' in the pp collisions with different energy scales. The solid curve is described by Eq. 1. The data points are taken from [8]. The inset shows the distribution of the ratio between the experimental data and the fitted results.

mechanism behind this scaling behavior, the model of percolation of strings is utilized [11]. In this model, color strings are stretched between the two colliding hadrons in the pp or $p\bar{p}$ collisions. These strings will split into new strings with the emission of $q\bar{q}$ pairs. Observed hadrons are formed through this quark pair emission. The transverse area of a color string is $S_1 = \pi r_0^2$, where $r_0 = 0.2$ fm. If there are n strings, they may overlap with each other and thus form a cluster with a transverse area of S_n . The p_T distribution at energy scale $\sqrt{s'}$ could be related to the p_T distribution at energy scale \sqrt{s} by a linear transformation on p_T at energy scale \sqrt{s} : $p_T \rightarrow p_T / ((nS_1/S_n) \sqrt{s} / (nS_1/S_n) \sqrt{s})^{1/4}$. Here nS_1/S_n gives the degree of string overlap. If strings just get in touch with each other, then $S_n = nS_1$ and $nS_1/S_n = 1$. If strings maximumly overlap with each other, then $S_n = S_1$ and $nS_1/S_n = n$ with $n > 1$. Comparing the p_T transformation in this model with the one used in the way to search for the scaling behavior, $p_T \rightarrow p_T/K$, we know that K gives the ratio between the degrees of string overlap for the collisions at $\sqrt{s'}$ and \sqrt{s} . For the pp ($p\bar{p}$) collisions at CMS (CDF), \sqrt{s} is set to be 7 (1.96) TeV and $\sqrt{s'}$ is set to be 0.9, 2.36 and 7 (0.63, 1.8 and 1.96) TeV. As described in Ref. [11], the degree of string overlap, nS_1/S_n , grows with the increase of the energy scale. Thus K should also grow with the increase of the energy scale. That's indeed what we observed in Tables I and II. And we found that in the pp ($p\bar{p}$) collisions the degrees of string overlap at $\sqrt{s'} = 0.9$ and 2.36 (0.63 and 1.8) TeV are about 33% and 60% (52% and 96%) of the degree of string overlap at $\sqrt{s} = 7$ (1.96) TeV. As a summary, with the model of percolation of strings, the scaling behavior we observed in the p_T distributions of charged hadrons produced at different energy scales is successfully explained.

ACKNOWLEDGMENTS

This work was supported by Shaanxi Normal University under Grant No. 801069. This work was also sup-

ported in part by the National Natural Science Foundation of China under Grant Nos. 11075061 and 11221504, by the Ministry of Education of China under Grant No. 306022, and by the Programme of Introducing Talents of Discipline to Universities under Grant No. B08033.

-
- [1] J. D. Bjorken and E. A. Paschos, Phys. Rev. **185**, 1975 (1969).
 - [2] R. C. Hwa and C. B. Yang, Phys. Rev. Lett. **90**, 212301 (2003).
 - [3] L. L. Zhu and C. B. Yang, Phys. Rev. C **75**, 044904 (2007).
 - [4] W. C. Zhang, Y. Zeng, W. X. Nie, L. L. Zhu, and C. B. Yang, Phys. Rev. C **76**, 044910 (2007).
 - [5] M. Praszalowicz, Phys. Rev. Lett. **106**, 142002 (2011).
 - [6] M. Rybczynski, Z. włodarczyk, and G. Wilk, J. Phys. G: Nucl. Part. Phys. **39**, 095004 (2012).
 - [7] C. Tsallis, Stat. Phys. **52**, 479 (1988); Eur. Phys. J. A **48**, 161 (2009); *Introduction to Nonextensive Statistical Mechanics* (Springer, 2009).
 - [8] V. Khachatryan *et al.* (CMS Collaboration), JHEP **02**, 041 (2010); Phys. Rev. Lett. **105**, 022002 (2010).
 - [9] F. Abe *et al.* (CDF Collaboration), Phys. Rev. Lett. **61**, 1819 (1988).
 - [10] T. Aaltonen *et al.* (CDF Collaboration), Phys. Rev. D **79**, 112005 (2009).
 - [11] M. A. Braun, F. del Moral, and C. Pajares, Phys. Rev. C **65**, 024907 (2002).